Application of the method of continued fractions to multichannel studies on electronic excitation of H_2 by electron impact

A. M. Machado
Instituto de Física de São Carlos, USP, 13560-970 São Carlos, São Paulo, Brazil

M. M. Fujimoto
Departamento de Física, UFPR, 81531-990 Curitiba, PR, Brazil

A. M. A. Taveira and L. M. Brescansin
Instituto de Física ''Gleb Wataghin,'' UNICAMP, 13083-970 Campinas, São Paulo, Brazil

M.-T. Lee
Departamento de Química, UFSCar, 13565-905 São Carlos, São Paulo, Brazil
(Received 5 September 2000; published 8 February 2001)

In the present work, the method of continued fractions at a five-channel close-coupling level of approximation is applied to study the low-energy electron-impact excitation in linear molecules. Particularly, cross sections for the $X^1\Sigma_g^+ \rightarrow b^3\Sigma_u^+$, $X^1\Sigma_g^+ \rightarrow a^3\Sigma_g^+$, and $X^1\Sigma_g^+ \rightarrow c^3\Pi_u$ transitions in H_2 in the (15–40)-eV energy range are reported. As in our early two-state studies, no orthogonality constraint between the bound and continuum orbitals is imposed and the one-electron exchange terms are considered explicitly. In general, our calculated cross sections are in good agreement with the results obtained by the four-state Kohn variational method. Comparison between our calculated results with available experimental data is encouraging.

DOI: 10.1103/PhysRevA.63.032707 PACS number(s): 34.80.Gs

I. INTRODUCTION

Cross sections for electron-molecule scattering play important role in many fundamental areas such as radiation science, plasma processes, astrophysics, studies of Earth's and planetary atmospheres, and so on [1]. Nevertheless, the measurement of reliable cross sections for electronic excitations in molecules remains a difficult challenge for researchers working in this area. On the theoretical side, the calculation of accurate cross sections for such processes is also far from satisfactory. Therefore, despite the significant progress achieved during the last two decades [2–4], to date there are still relatively few calculated values of electronic excitation cross sections reported in the literature, particularly for polyatomic molecules [5–7]. Moreover, even for a molecule as simple as H_2, despite the good agreement seen between the excitation cross sections at the two-state level of approximation calculated by different theoretical methods [2–4,8,9], results obtained using methods that include multichannel effects [such as the seven-state *R*-matrix method (RM-7S) [10,11], the four-state complex Kohn variational method (KV-4S) [12], and the Schwinger multichannel method [13]] have shown significant discrepancies when compared with each other and also with the available experimental data. All the above-mentioned multichannel methods make use of square-integrable functions to represent the continuum scattering orbitals. The discrepancies between their calculated results would reflect different physical assumptions in the calculations, such as the number of states taken into account, the orthogonality constraints between the bound and continuum orbitals, the electron correlation of the target, etc. Therefore, further systematic investigation on this matter is needed in order to better understand the dynamics of electron-impact excitation processes in molecules.

Recently, we have applied the method of continued fractions (MCF) to studies on low-energy electron-atom and electron-molecule interactions [14,15]. In particular, the MCF has been successfully applied to the calculations of cross sections for excitations from the ground state to the three lowest triplet states in H_2 at the two-state close-coupling level of approximation [8,9]. The MCF is a numerical method that solves iteratively the Lippmann-Schwinger scattering equation [16,17]. In this method, no basis functions are needed to describe the scattering orbitals and the converged scattering functions and reactance *K* matrices would correspond to the exact solutions for a given interaction potential. Our previous studies [15] have shown that the MCF is very efficient and converged *K* matrices can be obtained within few iterations. Our MCF computational code has now been extended to also account for multichannel interactions. In this work, this newly developed MCF program is applied to study electron-H_2 scattering at a four-state five-channel level (MCF-5C) of coupling. More specifically, cross sections for the excitations from the ground state to the $b^3\Sigma_u^+$, $a^3\Sigma_g^+$, and $c^3\Pi_u$ states by electron impact are reported in the (15–40)-eV range. These are exactly the same states retained in the KV-4S calculations of Parker *et al.* [12]. Nevertheless, there are some different physical aspects in the present and in their calculations. For instance, while in the KV-4S calculations the orthogonality between the bound and the continuum orbitals was imposed and the correlation terms such as $1\sigma_g 1\sigma_u^2$ and $1\sigma_g 1\pi_u^2$ were included to relax that constraint. In this study the orthogonality condition between the bound and the continuum orbitals is relaxed [8,9] and the one-electron exchange terms are taken into account explicitly. Therefore, comparison of present calculated results with available experimental and other calculated data,

particularly with those of KV-4S, would provide useful insight into the effects of multichannel interactions on the calculated cross sections.

The organization of this paper is as follows. In Sec. II we provide a brief discussion of the theory used in the present study. Some relevant computational details are also given in this section. Finally, the calculated differential and integral cross sections for excitations to $b^3\Sigma_u^+$, $a^3\Sigma_g^+$, and $c^3\Pi_u$ states are presented in Sec. III, where we also summarize our conclusions.

II. THEORY AND COMPUTATION

In the present study, the wave function $\Psi(1,\ldots,N+1)$ that describes the interaction between an electron and a molecule of N electrons is the solution of a Schrödinger equation of the form

$$(H-E)\Psi(1,\ldots,N+1)=0, \tag{1}$$

where

$$H=T+H_M+V_{int}, \tag{2}$$

T is the kinetic energy operator of the incident electron, H_M the Hamiltonian operator of the target, V_{int} the interaction potential operator, and E the total energy. The wave function that corresponds to a particular state α of the molecule is given by $\Phi_\alpha(1,\ldots,N)$ and satisfies the eigenvalue equation

$$H_M\Phi_\alpha(1,\ldots,N)=E_\alpha\Phi_\alpha(1,\ldots,N). \tag{3}$$

Equation (1) can be converted into a matrix-form Lippmann-Schwinger equation:

$$\tilde{\Psi}=\tilde{S}+\tilde{G}_0\tilde{U}\tilde{\Psi}, \tag{4}$$

where $\tilde{\Psi}$ is the solution of Eq. (1) in matrix form, $\tilde{S}$ is a diagonal matrix that represents a set of solutions of the $(N+1)$-electron unperturbed Schrödinger equation with matrix elements

$$S_{\alpha\alpha}=\Phi_\alpha e^{i\vec{k}_\alpha\cdot\vec{r}_{N+1}}, \tag{5}$$

$\tilde{G}_0$ is also a diagonal matrix representing the unperturbed Green's operator, and $\tilde{U}$ is the matrix of the reduced potential operator.

The application of the MCF consists basically of defining an nth-order ''weakened'' potential operator $\tilde{U}^{(n)}$ as

$$\tilde{U}^{(n)}=\tilde{U}^{(n-1)}-\tilde{U}^{(n-1)}|\tilde{S}^{(n-1)}\rangle(\tilde{A}^{(n-1)})^{-1}\langle\tilde{S}^{(n-1)}|\tilde{U}^{(n-1)}. \tag{6}$$

The nth-order correction of D matrix is defined through the relation

$$\tilde{D}^{(n)}=\tilde{B}^{(n)}+\tilde{A}^{(n)}[\tilde{A}^{(n)}-\tilde{D}^{(n+1)}]^{-1}\tilde{A}^{(n)}. \tag{7}$$

Here,

$$\tilde{A}^{(n)}=\langle\tilde{S}^{(n)}|\tilde{U}^{(n)}|\tilde{S}^{(n)}\rangle \tag{8}$$

and

$$\tilde{B}^{(n)}=\langle\tilde{S}^{(n-1)}|\tilde{U}^{(n-1)}|\tilde{S}^{(n)}\rangle, \tag{9}$$

where

$$\tilde{S}^{(n)}=\tilde{G}_0^P\tilde{U}^{(n-1)}\tilde{S}^{(n-1)}, \tag{10}$$

with the superscript P denoting the principal value of $\tilde{G}_0$. The reactance K matrix is related to the D matrix via

$$\tilde{K}=-\tilde{D}. \tag{11}$$

It is expected that $\tilde{U}^{(n)}$ defined in Eq. (6) becomes weaker and weaker with increasing n. As a result, the iterative procedure can be interrupted after some steps when the desired convergence is achieved. In practice, the nth-order D matrix can be obtained using Eq. (7) by setting $\tilde{D}^{(n+1)}=0$. Repeating the operation of Eq. (7), $\tilde{D}^{(n-1)}$, $\tilde{D}^{(n-2)}$, $\ldots$, $\tilde{D}^{(1)}$, and $\tilde{D}$ are obtained backwardly. The nth-iteration K matrix is then calculated via Eq. (11).

The transition T matrix is given by

$$\tilde{T}=-\frac{2\tilde{K}}{(1-i\tilde{K})} \tag{12}$$

and the body-frame scattering amplitude is related to this matrix via

$$f=-2\pi^2T. \tag{13}$$

In order to compare the calculated cross sections with the experimental data, a frame transformation on the scattering amplitude is made. The resulting laboratory-frame differential cross sections (DCSs), expanded in a j_t-basis representation [18] and averaged over the molecular orientations, have the form [19]

$$\frac{d\sigma}{d\Omega}(n\leftarrow 0)=P_sM_n\frac{k_f}{k_0}\sum_{j_tm_tm_t'}\frac{1}{(2j_t+1)}|B^{j_t}_{m_tm_t'}(n\leftarrow 0,\hat{r'})|^2, \tag{14}$$

where $\vec{j}_t=\vec{l}'-\vec{l}$ is the transferred angular momentum during the collision, and m_t' and m_t are the projections of j_t along the laboratory and molecular axis, respectively. The P_s factor results from summing over final and averaging over initial spin sublevels, and M_n is the orbital angular momentum projection degeneracy factor of the final target state. The quantity $k_0(k_f)$ is the magnitude of the linear momentum of the incoming (outgoing) electron.

In our calculation, the ground-state $(X^1\Sigma_g^+)$ target is represented by the configuration $1\sigma_g^2$ and the excited $b^3\Sigma_u^+$, $a^3\Sigma_g^+$, and $c^3\Pi_u$ states by $1\sigma_g1\sigma_u$, $1\sigma_g2\sigma_g$, and $1\sigma_g1\pi_u$ configurations, respectively. The $1\sigma_g$ orbital is generated at the Hartree-Fock level, while the $1\sigma_u$, $2\sigma_g$, and $1\pi_u$ orbitals are constructed as improved virtual orbitals [20], by diagonalizing the V_{N-1} potential of the core in the SCF basis. A $6s/4p$ uncontracted Cartesian Gaussian basis set of Huzi-

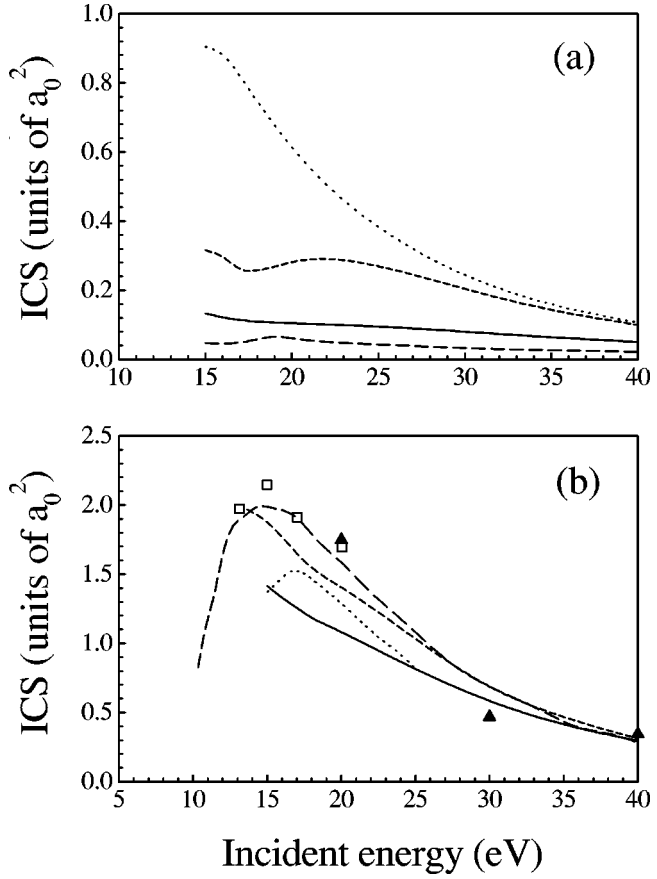

FIG. 1. (a) Partial contributions from overall symmetries to the ICSs for the $X^1\Sigma_g^+ \rightarrow b^3\Sigma_u^+$ excitation in H_2 by electron impact calculated using the MCF-5C. Solid line, contribution from the $^2\Sigma_g$ symmetry; short-dashed line, that from $^2\Sigma_u$; dashed line, that from $^2\Pi_g$; long-dashed line, that from $^2\Pi_u$. (b) ICSs for the $X^1\Sigma_g^+ \rightarrow b^3\Sigma_u^+$ excitation in H_2 by electron impact. Solid line, present MCF-5C results; long-dashed line, MCF-2C results of Lee *et al.* [8]; dashed line, KV-4S ICSs of Parker *et al.* [12]; short-dashed line, RM-7S data of Branchett *et al.* [11]; open squares, measured data of Nishimura and Danjo [25]; full triangles, measured data of Khakoo and Trajmar [24].

naga [21], augmented by three *s*- ($\alpha = 0.04$, 0.015, and 0.005) and five *p*- ($\alpha = 0.06$, 0.02, 0.009, 0.003, and 0.001) uncontracted functions, was used for these calculations. With this basis set, the calculated SCF energy at the equilibrium internuclear distance (1.4006 a_0) is $-1.133\,220$ a.u., to be compared with the Hartree-Fock limit [22] of -1.1336 a.u. The calculated vertical excitation energies for the transitions leading to the $b^3\Sigma_u^+$, $a^3\Sigma_g^+$, and $c^3\Pi_u$ states are 9.97, 12.027, and 12.307 eV, respectively. These values can be compared with the experimental ''vertical'' excitation energies of 10.027, 12.28, and 12.60 eV from the $\nu = 0$ vibrational level of the ground state for the same transitions. The zero-point vibrational energy is taken as 0.27 eV [23].

Furthermore, both the continuum wave function and the reactance *K* matrix expanded in a basis of irreducible representations of the $D_{\infty h}$ point group are block diagonal. In the present calculation, this partial-wave expansion is truncated at $l_{max} = 10$ and $m_{max} = 2$. Since only short-range interactions of exchange nature are involved in the transitions studied herein, the calculated cross sections converge to better than 2% using these truncation parameters. Also, convergence upto three significant digits in the *K*-matrix elements is achieved within six iterations for all the incident energies covered in the present study.

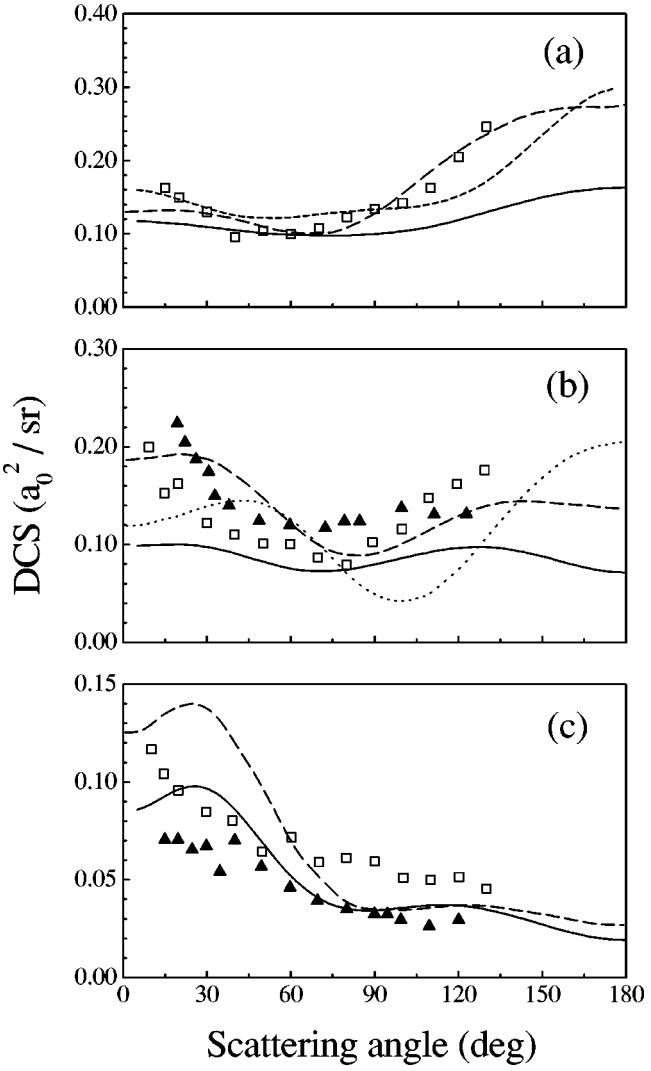

FIG. 2. DCSs for the $X^1\Sigma_g^+ \rightarrow b^3\Sigma_u^+$ excitation in H_2 by electron impact at (a) 15 eV, (b) 20 eV, and (c) 30 eV. The symbols are the same as in Fig. 1(b).

III. RESULTS AND DISCUSSION

A. The $X^1\Sigma_g^+ \rightarrow b^3\Sigma_u^+$ transition

In Fig. 1(a) we show our calculated partial contributions from the $^2\Sigma_g$, $^2\Sigma_u$, $^2\Pi_g$, and $^2\Pi_u$ overall scattering symmetries to the integral cross sections (ICSs) for the $X^1\Sigma_g^+ \rightarrow b^3\Sigma_u^+$ transition. Our results clearly show that the contribution from the $^2\Sigma_u$ scattering channel is dominant, followed by that from the $^2\Pi_g$ channel. Contributions from the $^2\Delta_g$ and $^2\Delta_u$ symmetries are too small and therefore are not shown. Figure 1(b) compares our MCF-5C ICSs with the RM-7S calculated results of Branchett *et al.* [10], with the

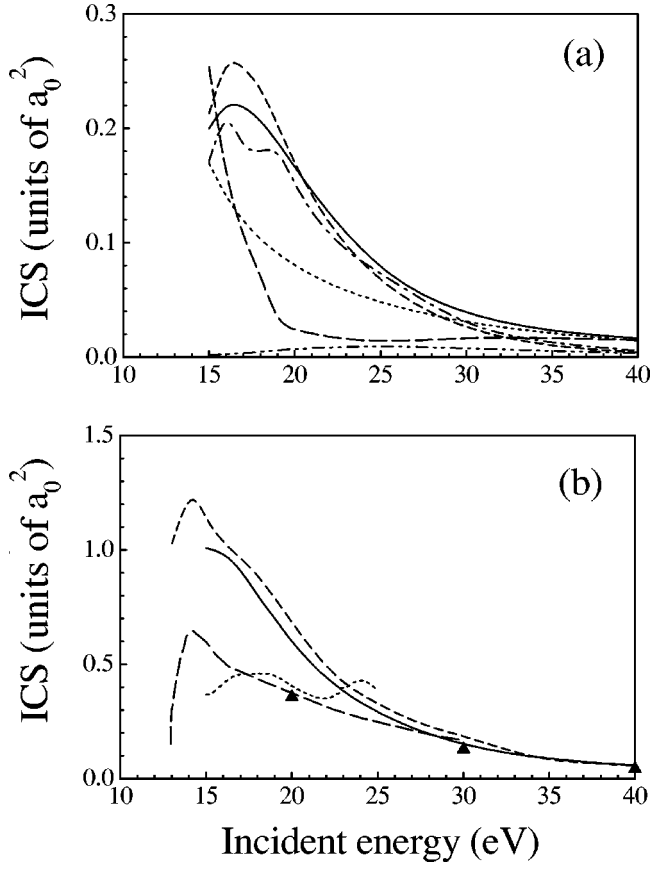

FIG. 3. (a) Same as Fig. 1(a), but for the $X^1\Sigma_g^+ \rightarrow a^3\Sigma_g^+$ transition. The symbols are the same as in Fig. 1(a) except as follows: dash-dotted line, the contribution from $^2\Delta_g$; and dashed–double-dotted line, that from the $^2\Delta_u$ overall symmetries. (b) Same as Fig. 1(b), but for the $X^1\Sigma_g^+ \rightarrow a^3\Sigma_g^+$ transition. The symbols are the same as in Fig. 1(b).

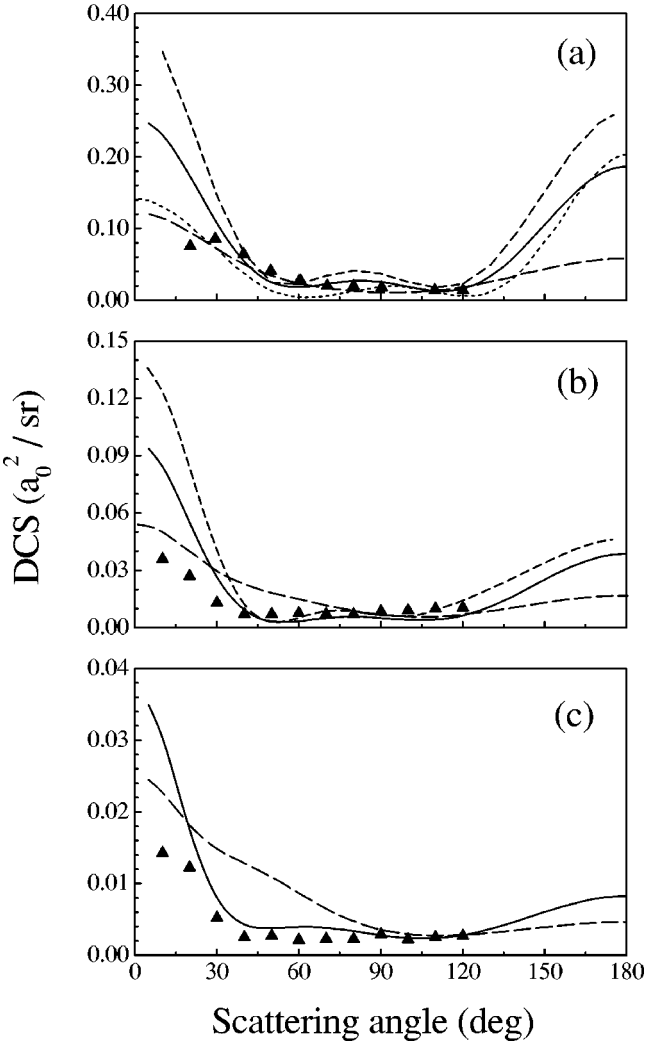

FIG. 4. DCSs for the $X^1\Sigma_g^+ \rightarrow a^3\Sigma_g^+$ excitation in H_2 by electron impact at (a) 20 eV, (b) 30 eV, and (c) 40 eV. The symbols are the same as in Fig. 1(b).

KV-4S results of Parker *et al.* [12] and with some available experimental data. Previous calculated results by the two-state MCF (MCF-2C) [8] are also shown. For energies below 35 eV, discrepancies are seen between the calculated ICSs at the MCF-2C and the MCF-5C levels of approximation. These differences illustrate the importance of the multichannel effects. Particularly for this transition, these effects lead to smaller excitation ICSs. Above that energy, the agreement between the MCF-2C ICSs and the MCF-5C ICSs is quite good reflecting that the interchannel coupling effects become smaller at high incident energies. On the other hand, our MCF-5C ICSs agree with the results of RM-7S [10] and KV-4S [12] within 20% in the entire energy range where the comparison is made. This agreement is encouraging, even considering the different physical aspects inherent in these methods. Moreover, the comparison with the available experimental results [24,25] reveals that our MCF-5C ICSs lie below these data at the lower end of the incident energies. However, quite good agreement with the measured data of Khakoo and Trajmar [24] is seen at 30 and 40 eV.

In Figs. 2(a)–2(c) we show our calculated MCF-5C DCSs and the previous MCF-2C DCSs [8] for the $X^1\Sigma_g^+ \rightarrow b^3\Sigma_u^+$ transition at 15, 20, and 30 eV, respectively, along with some experimental data available in the literature [24,25]. The calculated results of KV-4S [12] at 15 eV and the RM-7S DCSs [11] at 20 eV are also shown for comparison. As expected, the differences seen between our calculated DCSs by the MCF-5C and the MCF-2C are due to the multichannel effects. Nevertheless, the agreement between these two MCF calculations improves with increasing incident energies. At 15 eV, our MCF-5C DCSs agree qualitatively well with those of KV-4S. The quantitative agreement is fair, being the KV-4S DCSs systematically above our MCF-5C data. At 20 eV, our results disagree strongly with the calculated RM-7S DCSs of Branchett *et al.* [11], both in shape and magnitude. This discrepancy is somehow expected, since in their calculation three lowest singlet excited states were also included. Besides, they have also constrained the scattering wave functions to be orthogonal with the bound orbitals. Comparing our results with the experiments, it is seen that in general there is a qualitative agreement. Quantitatively, the agreement is fair, except at 30 eV, where our calculated results are in good agreement with the measured data, both qualitatively and quantitatively.

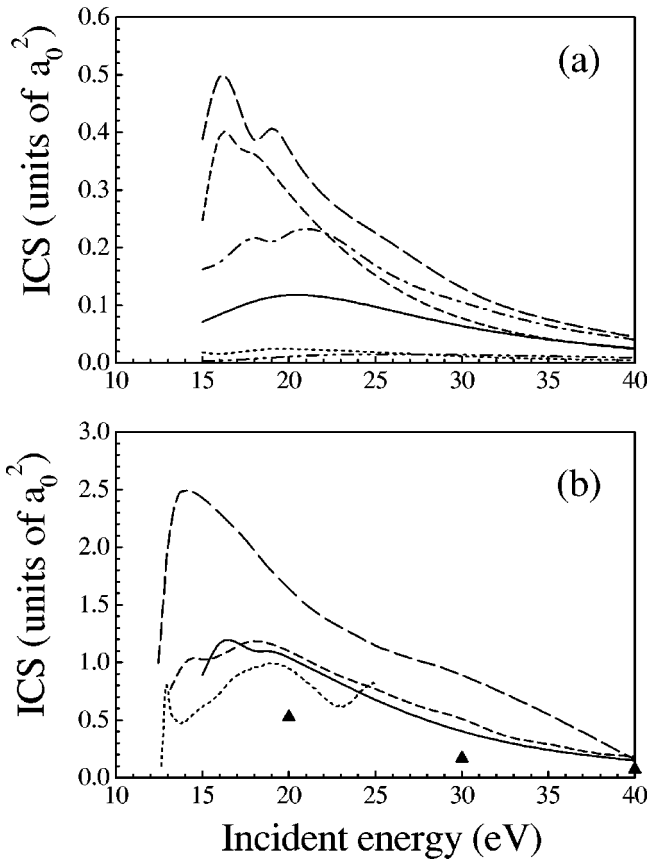

FIG. 5. (a) Same as Fig. 2(a), but for the $X^1\Sigma_g^+ \rightarrow a^3\Sigma_g^+$ transition. The symbols are the same as in Fig. 2(a).

B. The $X^1\Sigma_g^+ \rightarrow a^3\Sigma_g^+$ transition

In Fig. 3(a) we show the partial contributions to the ICSs from the first six scattering symmetries calculated with the MCF-5C for the $X^1\Sigma_g^+ \rightarrow a^3\Sigma_g^+$ transition in H_2. For this transition, the contributions from the $^2\Sigma_g$, $^2\Pi_g$, and $^2\Delta_g$ symmetries are equally important. The contribution from $^2\Pi_u$ is also important at low incident energies. In Fig. 3(b) we compare our MCF-5C ICSs with those calculated using the KV-4S and RM-7S and the experimental results of Khakoo and Trajmar [24]. Previous MCF-2C data [9] are also included for comparison. The MCF-5C ICSs agree very well with those of KV-4S over the energy range covered herein, whereas the RM-7S ICSs lie in general below our data. Furthermore, our MCF-2C ICSs also lie systematically below the MCF-5C data for incident energies below 25 eV. Above this energy, a very good agreement is seen between these two sets of results, which indicates again that the interchannel-coupling effects are small at high energies. The MCF-5C ICSs also agree very well with the experimental data of Khakoo and Trajmar at 30 and 40 eV. At 20 eV, our calculation overestimates the ICSs.

Figures 4(a)–4(c) show the calculated MCF-5C DCSs for the $X^1\Sigma_g^+ \rightarrow a^3\Sigma_g^+$ transition at 20, 30, and 40 eV, respectively, along with the experimental data of Khakoo and Trajmar [24] and the calculated KV-4S DCSs of Parker *et al.* [12] at 20 and 30 eV and RM-7S results of Branchett *et al.* at 20 eV [11]. Our MCF-2C results [9] are also shown for comparison. For this transition, the multichannel-coupling effects are very important and lead to a strong increase of the DCSs at the forward and backward scattering directions, particularly at 20 eV. Also, the MCF-5C DCSs show a double-minimum structure at around 60° and 120°, which clearly indicates the dominant *d*-wave ($l=2$) scattering. Since this structure is also seen in the DCSs calculated using the KV-4S and RM-7S but is not seen in the MCF-2C DCSs, it results from the interchannel couplings. Quantitatively, our MCF-5C DCSs lie between those of the KV-4S and the RM-7S at 20 eV. Our calculated results also agree well with the experiment [24] at angles above 30°.

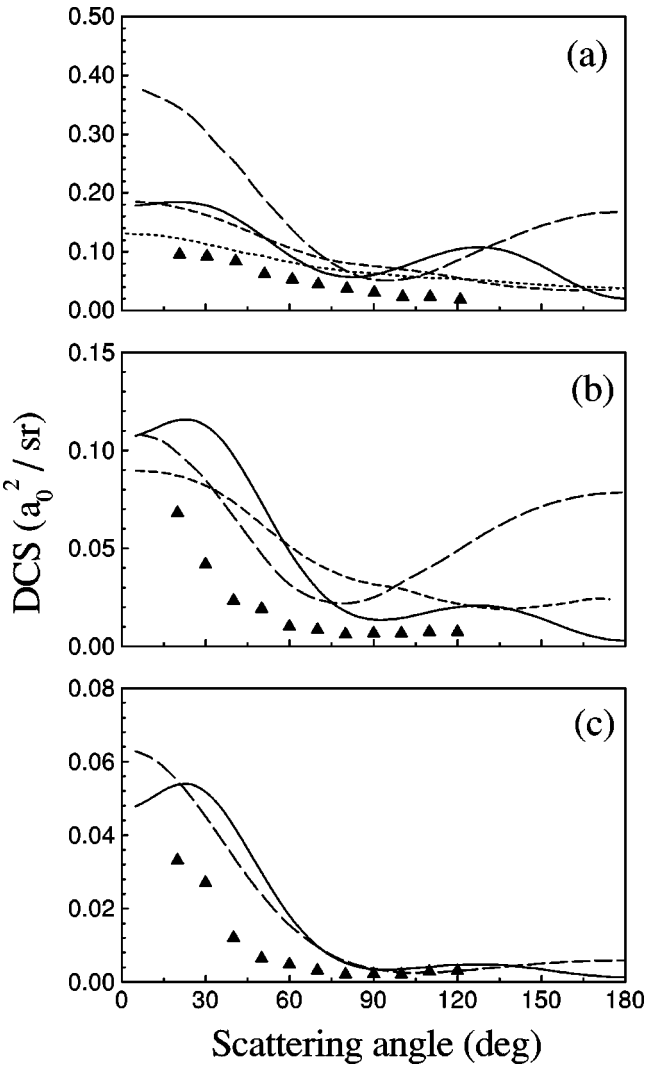

FIG. 6. DCSs for the $X^1\Sigma_g^+ \rightarrow c^3\Pi_u^+$ excitation in H_2 by electron impact at (a) 20 eV, (b) 30 eV, and (c) 40 eV. The symbols are the same as in Fig. 1(b).

C. The $X^1\Sigma_g^+ \rightarrow c^3\Pi_u$ transition

Figure 5(a) shows our MCF-5C partial contributions to the ICSs from the first six scattering symmetries for the $X^1\Sigma_g^+ \rightarrow c^3\Pi_u$ transition in H_2 by electron impact. For this transition, the contributions from the $m=1$ scattering channels are the most important, followed by $^2\Delta_g$ and $^2\Sigma_g$ chan-

nels. Figure 5(b) compares the ICSs calculated by using the MCF-5C, MCF-2C, KV-4S, and RM-7S with the experimental results of Khakoo and Trajmar [24]. There is a good agreement among the three calculations in which the multichannel effects are accounted for, although all calculations overestimate the experimental ICSs.

In Figs. 6(a)–6(c) we compare our calculated MCF-5C DCSs for the $X^1\Sigma_g^+ \rightarrow c^3\Pi_u$ transition at 20, 30, and 40 eV, respectively, with the previous MCF-2C DCSs [9] and the experimental data of Khakoo and Trajmar [24]. The calculated data of RM-7S at 20 eV and KV-4S at 20 and 30 eV are also shown for comparison. In general, the multichannel coupling reduces the calculated excitation DCSs for this transition at 20 and 30 eV, but does not affect significantly the calculated DCSs at 40 eV. Comparison with the experiment of Khakoo and Trajmar [24] shows a general qualitative agreement, although at 20 eV our MCF-5C DCSs show oscillations that are not seen in the experimental data. Quantitatively, the calculations systematically overestimate the magnitude of DCSs, although the discrepancy decreases with increasing incident energies. Comparing our MCF-5C DCSs with those of RM-7S and KV-4S, it is seen that at 20 eV, the RM-7S DCSs is in better agreement with the measured data. On the other hand, our MCF-5C DCSs oscillate around the KV-4S results at 20 and 30 eV.

In summary, this work reports a theoretical study on electronic excitation of H_2 by low-energy electron impact. DCSs and ICSs in the (15–40)-eV range for transitions leading to three lowest triplet states of the target are calculated in a five-channel level of approximation. The significant discrepancy seen between the MCF-5C results and previous MCF-2C data reveals the importance of the inclusion of multichannel effects in the calculations. In general, these effects become less relevant with increasing energies. On the other hand, despite of being formally very different, our calculated MCF-5C ICSs and DCSs agree generally well with those obtained by the KV-4S. Some small discrepancies are attributed to different physical aspects inherent in the two methods. The agreement between the present DCSs and the RM-7S results is fair. Indeed, this fact is somehow expected and several aspects aforementioned can be responsible for the disagreement between the results of the two calculations. In order to compare with their results, we are now planning to perform a seven-state nine-channel MCF calculation.

ACKNOWLEDGMENTS

This research was partially supported by the Brazilian Agencies CNPq, FAPESP, and FINEP-PADCT. A.M.M. thanks FAPESP.

[1] L. Pitchford, V. McKoy, A. Chutjian, and S. Trajmar, in *Swarm Studies and Inelastic Electron-Molecule Collisions*, Proceedings of the Meeting of the Fourth International Swarm and the Inelastic Electron-Molecule Collisions Symposium, edited by L. Pitchford, V. McKoy, A. Chutjian, and S. Trajmar (Springer-Verlag, New York, 1986).
[2] K. L. Baluja, C. J. Noble, and J. Tennyson, J. Phys. B **18**, L851 (1985).
[3] B. I. Schneider and L. A. Collins, J. Phys. B **18**, L857 (1985).
[4] M. A. P. Lima, T. L. Gibson, W. M. Huo, and V. McKoy, J. Phys. B **18**, L865 (1985).
[5] H. P. Pritchard, V. McKoy, and M. A. P. Lima, Phys. Rev. A **41**, 546 (1990).
[6] T. N. Rescigno and B. I. Schneider, Phys. Rev. A **45**, 2894 (1992).
[7] Q. Sun, C. Winstead, V. McKoy, and M. A. P. Lima, J. Chem. Phys. **96**, 3531 (1992).
[8] M.-T. Lee, M. M. Fujimoto, T. Kroin, and I. Iga, J. Phys. B **29**, L425 (1996).
[9] M.-T. Lee, M. M. Fujimoto, and I. Iga, J. Mol. Struct.: THEOCHEM **432**, 197 (1998).
[10] S. E. Branchett, J. Tennyson, and L. A. Morgan, J. Phys. B **23**, 4625 (1990).
[11] S. E. Branchett, J. Tennyson, and L. A. Morgan, J. Phys. B **24**, 3479 (1991).
[12] S. D. Parker, C. W. McCurdy, T. N. Rescigno, and B. H. Lengsfield III, Phys. Rev. A **43**, 3514 (1991).
[13] C. S. Sartori and M. A. P. Lima, in *Scientific Program and Abstract of Contributed Papers, XIX ICPEAC*, edited by J. B. A. Mitchell, J. W. McConkey, and C. E. Brion (Whistler, Canada, 1995), p. 28.
[14] M.-T. Lee, I. Iga, M. M. Fujimoto, and O. Lara, J. Phys. B **28**, L299 (1995).
[15] M.-T. Lee, I. Iga, M. M. Fujimoto, and O. Lara, J. Phys. B **28**, 3325 (1995).
[16] J. Horáček and T. Sasakawa, Phys. Rev. A **28**, 2151 (1983).
[17] J. Horáček and T. Sasakawa, Phys. Rev. A **30**, 2274 (1984).
[18] U. Fano and D. Dill, Phys. Rev. A **6**, 185 (1972).
[19] A. W. Fliflet and V. McKoy, Phys. Rev. A **21**, 1863 (1980).
[20] W. A. Goddard III and W. J. Hunt, Chem. Phys. Lett. **24**, 464 (1974).
[21] S. Huzinaga, J. Chem. Phys. **42**, 1293 (1965).
[22] W. Kolos and C. C. J. Roothaan, Rev. Mod. Phys. **32**, 219 (1960).
[23] M. A. P. Lima, T. L. Gibson, V. McKoy, and W. M. Huo, Phys. Rev. A **38**, 4527 (1988).
[24] M. A. Khakoo and S. Trajmar, Phys. Rev. A **34**, 146 (1986).
[25] H. Nishimura and A. Danjo, J. Phys. Soc. Jpn. **55**, 3031 (1986).